

Design and Development of a General Purpose 7 DOF Haptic Device

Gregory Tholey[†]

Program for Robotics, Intelligent Sensing, and Mechatronics
(PRISM) Laboratory[†]
Drexel University

Jaydev P. Desai^{*§}

Program for Robotics, Intelligent Sensing, and Mechatronics
(PRISM) Laboratory[†]
Drexel University

ABSTRACT

A seven degree-of-freedom (DOF) haptic device has been developed with applications towards robot-assisted minimally invasive surgery. The device consists of four degrees of force feedback (X, Y, Z, and grasping) capability and seven degrees of freedom for positioning capability. The haptic device is a closed kinematic chain with two halves (user interface and spatial mechanism) connected by a universal joint. Kinematic analysis of the haptic device has been developed with the particular goal of computing the slave robot position and the end point configuration of the laparoscopic tool. Additionally, the achievable workspace of the mechanism has been calculated based on the motion of each half of the device. Friction modeling and its compensation has also been presented to enable higher transparency of the haptic device.

CR Categories: J.2 [Physical Science and Engineering]

Keywords: haptic, minimally invasive surgery, robotic surgery, surgical simulation

1 INTRODUCTION

Development within the field of haptics has had significant advancement within the last couple of decades. Specifically, development of haptic interfaces with applications in the medical field for robotically-assisted procedures has produced many new haptic devices [1-5], as well as, the necessary surgical tools with appropriate sensors to be used with the haptic devices [6-18]. These devices may serve as haptic interfaces for multiple procedures or serve a single specific medical need. However, most of these haptic devices have one of the basic designs of manipulators; serial, parallel, or glove-type devices; each of which have their own advantages and disadvantages. Serial mechanisms have the benefit of a large workspace; however lack a sufficient force feedback capability without larger actuators that add significant weight. Parallel mechanisms can produce a high force output; however, they have a smaller workspace and limited maneuverability which may not be desirable in some surgical procedures. Glove-type haptic interface, similar to serial mechanisms, offer a large workspace but are even more limited

* corresponding author

[†] mailing address: PRISM Laboratory, 3141 Chestnut St., MEM Dept., Room 2-115, Philadelphia, PA 19104, USA

[‡] e-mail: gtholey@coe.drexel.edu

[§] e-mail: desai@coe.drexel.edu

in their force feedback capability as the weight of the actuators is typically carried by the user unless the haptic device is grounded. Therefore, incorporating the advantages of each of these types of haptic devices into a single design could help to improve the characteristics of the haptic device, especially in the area of robot-assisted surgery where a sufficiently large workspace and force output along with grasping feedback are desirable. In addition, the disadvantages of the various types could be minimized.

Based on this motivation, we have designed and developed a seven degree-of-freedom haptic device with four degrees of force feedback capability that has specific applications to robotically-assisted minimally invasive surgery (MIS). The haptic device consists of a closed kinematic chain that contains two halves; namely, the user interface and the spatial force feedback mechanism, which are connected together via a universal joint. The user interface has four degrees of freedom (roll, pitch, yaw, and linear translation) along with a grasping/dissecting interface for soft-tissue manipulation. This user interface allows the user to insert their hand and forearm in the device while inserting their fingers into two thimbles in the user interface. The interface then provides force feedback to the fingers in the thimbles for grasping/parting tasks and three dimensional force feedback to the user's hand and forearm via the attached spatial force feedback mechanism. The spatial force feedback mechanism has three orthogonal axes that are assembled in series for positioning and force reflection to the user interface via the universal joint. Previous work has focused on the initial design of this haptic device [19]. However, this paper presents a completely developed seven degree of freedom haptic device with friction estimation for the individual actuated joints as well as the kinematic analysis for the mechanism to facilitate end point control of the laparoscopic tool attached to the end-effector of the slave robot.

This paper is divided into the following sections. In section 2, we present the design of the haptic device along with the kinematics and workspace of the device. In section 3, we estimate the friction in the various actuated joints. Section 4 presents concluding remarks including our future work in this area.

2 MATERIALS AND METHODS

2.1 Design and Development

Our haptic device was designed specifically towards applications within robot-assisted MIS, however, it can also be used in other areas such as the automotive industry, gaming industry, rehabilitation aid for people with finger, hand, and/or forearm injuries, etc. This device is part of an overall haptic surgical system that we envision building (see Fig. 1). Through the haptic

device, we will be able to control the robot arm with attached surgical tool that is capable of measuring the forces at the end effector in 3D [20]. The user interface (see Fig. 2) of the haptic device will control the slave robot arm such as the Mitsubishi PA-10. The surgical tool attached to the robot arm can measure and feedback forces to the haptic device to reflect them to the user through the spatial force feedback mechanism (see Fig. 2), which would include forces in X, Y, and Z direction, in addition to the grasping forces through the grasping mechanism (θ) (see Fig. 3).

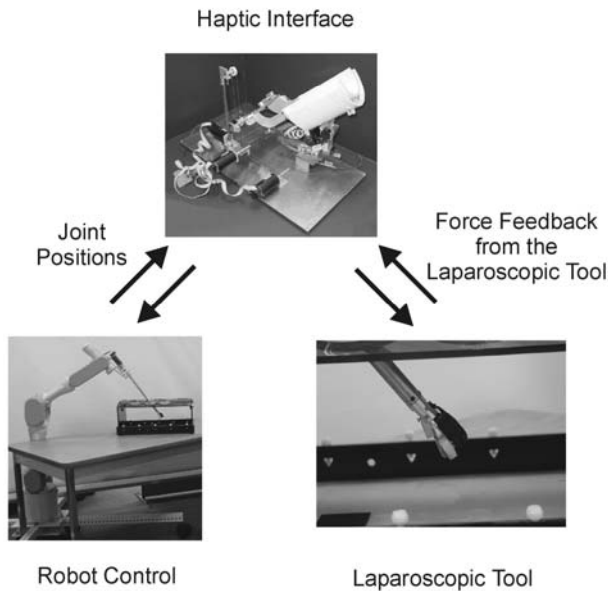


Figure 1: Schematic of the overall role of the haptic feedback system for laparoscopic surgery.

Several constraints were considered in the design process. The first constraint was the creation of an ergonomic design that conforms to the surgeon's motions during a medical procedure. Therefore, considering a surgeon's hand and arm, there are five general movements that consist of grasping/cutting/dissecting tissue using two fingers, roll, pitch, and yaw of the wrist, and the linear motion of the forearm for translation. All of these motions needed to be incorporated into the haptic device to replicate the surgeon's natural motions and thus increase the transparency of the device. Second, we needed to consider the location of force feedback in our device. In any typical MIS surgical procedure involving grasping, cutting, or dissecting, the forces are felt at the laparoscopic tool tip, where the surgical tool interacts with the soft-tissue. Therefore, it is desirable to produce a similar force feedback capability through the haptic device. Other important design considerations were backdriveability, low friction, high transparency, adequate force ranges, static balancing, and a large workspace.

The device consists of a closed kinematic chain with two halves; a user interface and a spatial force feedback mechanism (see Fig. 2). The user interface consists of an arm rest with four degrees-of-freedom position feedback (roll, pitch, yaw, and linear motion of the arm rest) and a grasping/dissecting mechanism at the end of the arm rest. Therefore, a user could insert their hand and forearm into the user interface and use the haptic device as a master device for controlling a slave robot,

while receiving force feedback. The joints of the user interface proceed from the base → yaw joint → prismatic joint → pitch joint → roll joint → end effector joint (universal joint). All of these joints, except for the prismatic joint, are equipped with encoders for tracking the position of the user interface (see Table 1 for joint limits). The position of the prismatic joint can be determined from the position of the other three joints and the spatial force feedback mechanism joints. The grasping/dissecting mechanism contains two thimbles for the user's fingers (thumb and index finger, for example) that are coupled to a DC motor with an encoder. This allows the user to fully control a grasping mechanism, such as a laparoscopic tool at the end of a robotic surgical system, and also receive force feedback as measured by sensors in the laparoscopic tool as developed in [16]. The spatial force feedback mechanism consists of a three degree-of-freedom positioning stage that attaches to the user interface at the grasping mechanism through the use of a universal joint (see Table 1 for joint limits). This mechanism was designed to provide force feedback in three directions through orthogonally-mounted linear actuators. Therefore, this force feedback mechanism can relay manipulation forces, such as the pulling or pushing of an object (e.g. soft tissue in MIS), to the user in addition to the gripping forces felt through the grasping mechanism. This mechanism was designed to apply all forces to the user at the grasping mechanism rather than through the joints of the arm rest. This enhances the transparency of the haptic device by providing feedback to the user, which is more analogous to conventional open surgery where the surgeon primarily receives feedback at the point of contact with the soft tissue and/or organs.

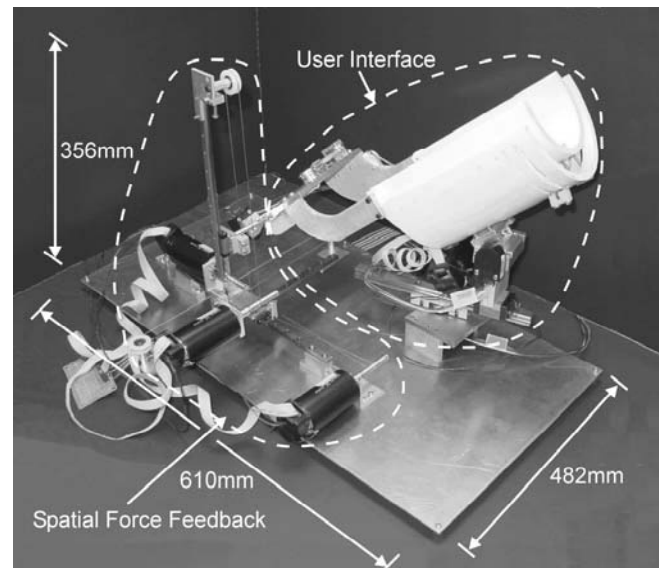


Figure 2: Prototype of the haptic device.

The range of forces for each axis of feedback was designed for general manipulation tasks and also robot-assisted MIS. However, weight and inertia properties of the actuators must also be considered. Previous research has attempted to define the range of forces that are felt during laparoscopic and conventional surgeries. For a typical palpation task, the average magnitude of force was 12.5N [3]. Another research experiment found grasping forces of similar magnitude with a maximum force of approximately 16N and a maximum pulling force (along the shaft of the laparoscopic tool) of approximately 17N [21]. Similar

results were also reported by Baumann [2] and Gupta [22]. Therefore, we decided to use these experimental results as general guidelines for the magnitude of force feedback along the three spatial (X,Y,Z) and grasping direction (θ).

Table 1: Joint limits for the haptic device

Joint	Range of motion
User Interface	
Yaw joint	0° to 180°
Prismatic joint	-76.2mm to 76.2mm
Pitch joint	0° to 20°
Roll Joint	-35° to 35°
Spatial Force Feedback Mechanism	
Prismatic joint 1 (X axis)	0mm to 223mm
Prismatic joint 2 (Y axis)	0mm to 223mm
Prismatic joint 3 (Z axis)	0mm to 183mm

In the design of the spatial force feedback mechanism, we used a cable-driven transmission powered by DC motors to actuate the prismatic joints. Each of the motors uses a 6.35 mm diameter grooved pulley on its shaft with one (X and Z axes) or two (Y axis) idle pulleys at the limits of travel. We selected brushed DC motors with encoders (RE40 manufactured by Maxon Motors) for each axis. The DC motor is capable of providing up to 181 mNm of continuous torque, which equates to approximately 56N of force. However, frictional losses reduce this number to approximately 40N (as measured experimentally).

The grasping/parting force feedback mechanism also uses a cable-driven transmission powered by a DC motor; however, the transmission involves two stages (see Fig. 3). This two stage transmission allows the placement of the motor close to the pitch axis of the user interface to reduce the moment on that axis. The DC motor has a 6.35mm diameter pulley mounted to its shaft with a steel cable that transmits the force to an intermediate pulley that is 19mm in diameter. Connected to this pulley is a

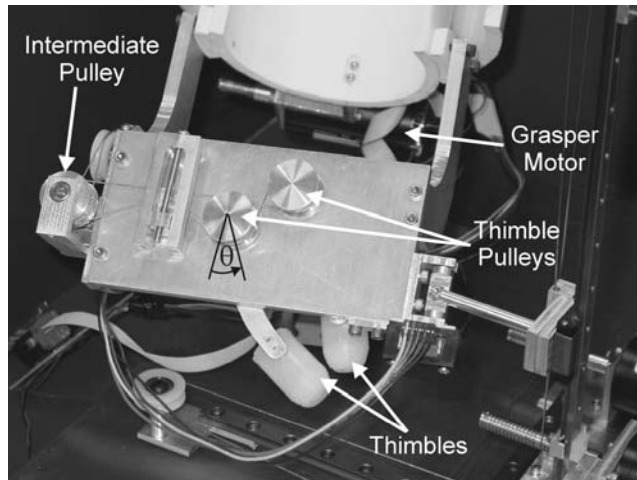


Figure 3: Details of the grasping mechanism.

6.35mm diameter pulley that transmits the motion further to a 19mm diameter pulley, to which the thimbles are attached. This transmission represents an increase in torque of 9:1 from the motor pulley to the thimble pulley. The brushed DC motor with encoder (RE36 manufactured by Maxon Motors) is capable of

producing up to 88.8mNm of continuous torque. This equates to approximately 12.5N of force at the tip of the thimbles as desired from research in the literature.

2.2 Kinematics

The haptic device is designed as a closed kinematic chain with a universal joint connecting the spatial force feedback mechanism to the user interface. Therefore, the kinematics of the haptic device can be decoupled into two separate halves that both end at the universal joint (see Fig. 4). These kinematic equations can then be used to find the position of the prismatic joint on the user interface. The position of the prismatic joint can be mapped to the corresponding translation of the end-effector of the slave robot in the global

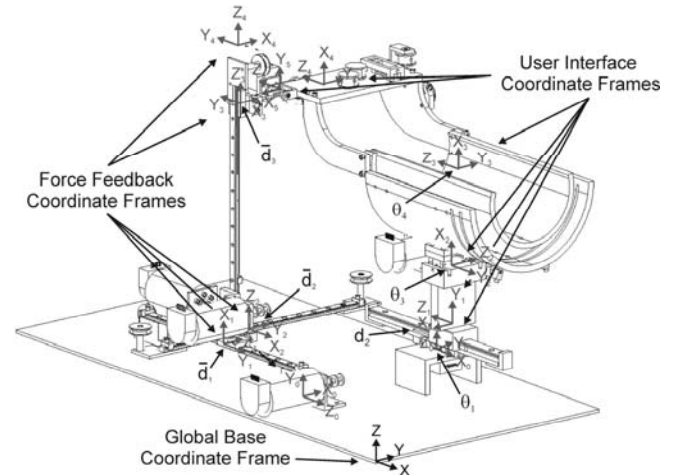


Figure 4: Coordinate frames for the user interface and spatial force feedback mechanism.

coordinate frame (mapping not described in this paper). The movement of the grasping mechanism correlates to the opening/closing of the jaws of the laparoscope. Starting with the forward kinematics of the user interface, we placed coordinate frames on both halves of the haptic device (see Fig. 4). Next, we obtained the D-H parameters of each half that are shown in Table 2 and Table 3.

Table 2: D-H parameters for the user interface

Joint	θ	α	a (mm)	d (mm)
1	$\theta_1 - \pi/2$	$\pi/2$	0	38.583
2	$\pi/2$	$-\pi/2$	66.675	d_2
3	θ_3	$\pi/2$	109.55	0
4	θ_4	0	53.772	192.34
5	$-\pi/2$	0	82.98	0

Table 3: D-H parameters for the spatial force feedback mechanism

Joint	θ	α	a (mm)	d (mm)
1	$\pi/2$	$\pi/2$	36.627	\bar{d}_1
2	$\pi/2$	$\pi/2$	0	\bar{d}_2
3	$\pi/2$	0	0	\bar{d}_3
4	0	0	57.633	0

The transformation matrix relating coordinate transformation from one joint to the next is given by:

$$T_i^{i-1} = \begin{bmatrix} \cos(\theta_i) & -\sin(\theta_i)\cos(\alpha_i) & \sin(\theta_i)\sin(\alpha_i) & a_i \cos(\theta_i) \\ \sin(\theta_i) & \cos(\theta_i)\cos(\alpha_i) & -\cos(\theta_i)\sin(\alpha_i) & a_i \sin(\theta_i) \\ 0 & \sin(\alpha_i) & \cos(\alpha_i) & d_i \\ 0 & 0 & 0 & 1 \end{bmatrix} \quad (1)$$

where T_i^{i-1} represents the homogeneous transformation matrix from the i^{th} frame to the $(i-1)^{\text{th}}$ frame on the user interface side. By pre-multiplying the homogeneous transformation matrices for successive coordinate transformations, we can the transformation matrix for the end-effector as seen in the base frame, namely T_5^0 .

$$T_5^0 = T_1^0 T_2^1 T_3^2 T_4^3 T_5^4 \quad (2)$$

Similarly, for the spatial mechanism:

$$\bar{T}_4^0 = \bar{T}_1^0 \bar{T}_2^1 \bar{T}_3^2 \bar{T}_4^3 \quad (3)$$

where \bar{T}_i^{i-1} represents the homogeneous transformation matrix between successive frames on the spatial force feedback side. Based on the general definition of the homogeneous transformation matrix given by:

$$T = \begin{bmatrix} R_{11} & R_{12} & R_{13} & d_1 \\ R_{21} & R_{22} & R_{23} & d_2 \\ R_{31} & R_{32} & R_{33} & d_3 \\ 0 & 0 & 0 & 1 \end{bmatrix} \quad (4)$$

we can obtain the displacement vector, $\vec{D} = [d_1, d_2, d_3]^T$, for the location of the universal joint in the base coordinate frame. As a result:

$$\vec{D} = \begin{bmatrix} -a_5 S_1 S_3 S_4 + a_5 C_1 C_4 - a_4 S_1 S_3 C_4 \\ -a_4 C_1 S_4 + d_4 S_1 C_3 - a_3 S_1 S_3 + S_1 d_2 - 177.8 \\ a_5 C_1 S_3 S_4 + a_5 S_1 C_4 + a_4 C_1 S_3 C_4 \\ -a_4 S_1 S_4 - d_4 C_1 C_3 + a_3 C_1 S_3 - C_1 d_2 + 228.6 \\ 105.26 + a_5 C_3 S_4 + a_4 C_3 C_4 + d_4 S_3 + a_3 C_3 \end{bmatrix} \quad (5)$$

and

$$\vec{\bar{D}} = \begin{bmatrix} -8.523 + \bar{d}_1 \\ 5.622 + \bar{d}_2 \\ 1.442 + \bar{d}_3 \end{bmatrix} \quad (6)$$

where \vec{D} and $\vec{\bar{D}}$ relate to the displacement vector of the universal joint in base frame coordinates as viewed from the user interface and spatial force feedback side respectively. Since \vec{D} and $\vec{\bar{D}}$ are equal (as they refer to the same end effector location (universal joint)), by knowing the values of the yaw (θ_1), pitch (θ_3), and roll (θ_4) (based on the encoder readings) of the user interface displacement matrix (Eq. (5)) and the values of \bar{d}_1 , \bar{d}_2 , and \bar{d}_3 (based on the encoder readings) of the spatial force

feedback mechanism (Eq. (6)), we can calculate the position of the prismatic joint on the user interface. Further, the inverse kinematics of the spatial force feedback mechanism was developed from the displacement matrix (see Eq. (6)) to yield the joint positions based on the end-effector position given by:

$$\begin{bmatrix} \bar{d}_1 \\ \bar{d}_2 \\ \bar{d}_3 \end{bmatrix} = \begin{bmatrix} d_x + 8.523 \\ d_y - 5.622 \\ d_z - 1.442 \end{bmatrix} \quad (7)$$

where d_x , d_y , and d_z are the displacements of the end-effector with respect to the global coordinate frame.

The Jacobian relating the joint velocities to the end-effector velocity is given by:

$$\begin{bmatrix} J_{Li} \\ J_{Ai} \end{bmatrix} = \begin{cases} \begin{bmatrix} u_{i-1} \\ 0 \end{bmatrix} & \text{for a prismatic joint} \\ \begin{bmatrix} u_{i-1} \times r_{i-1,e} \\ u_{i-1} \end{bmatrix} & \text{for a rotational joint} \end{cases} \quad (8)$$

where J_{Li} is the linear velocity vector, J_{Ai} is the angular velocity vector, u_{i-1} is the unit vector along joint axis i , and $r_{i-1,e}$ is the position vector from joint $i-1$ to the end-effector as expressed in the global coordinate frame. Since we only have prismatic joints in the spatial force feedback mechanism, we need to calculate u_{i-1} using the homogeneous coordinate transformation matrices from joint i to joint $i-1$ given by the equations:

$$U_i = \begin{bmatrix} \cos(\theta_i) & -\sin(\theta_i) & 0 \\ \sin(\theta_i) & \cos(\theta_i) & 0 \\ 0 & 0 & 1 \end{bmatrix} \quad (9)$$

$$V_i = \begin{bmatrix} 1 & 0 & 0 \\ 0 & \cos(\alpha_i) & -\sin(\alpha_i) \\ 0 & \sin(\alpha_i) & \cos(\alpha_i) \end{bmatrix} \quad (10)$$

where U_i is the rotation about the joint's Z axis (θ_i), and V_i is the rotation about the joint's X axis (α_i). Using these equations, we can define the unit vector u_{i-1} using the following equation:

$$u_{i-1} = (U_0 V_0 U_1 V_1 \dots U_{i-1} V_{i-1}) \begin{bmatrix} 0 \\ 0 \\ 1 \end{bmatrix} \quad (11)$$

Solving for the unit vectors for each of the three joints of the spatial mechanism (using Eq. (11)) yields the Jacobian, J :

$$J = \begin{bmatrix} 0 & 1 & 0 \\ 0 & 0 & 1 \\ 1 & 0 & 0 \\ 0 & 0 & 0 \\ 0 & 0 & 0 \\ 0 & 0 & 0 \end{bmatrix} \quad (12)$$

As expected, the velocities of the joints are independent of the other actuated joints and therefore, the velocity of the end effector along an axis is equal to the velocity of the actuated joint along the same axis.

2.3 Workspace

The reachable workspace of the haptic device is the intersection of the workspace of the user interface half and the workspace of the spatial force feedback mechanism. Therefore, we developed an algorithm to determine this volume to verify the reachable workspace of the haptic device was sufficient for the range of motion in MIS procedures.

In order to determine the workspace, we started with analyzing the workspaces of the user interface and spatial force feedback mechanism separately. We approached this analysis by developing Matlab code using the kinematics to track the end effector position in the global coordinate frame. During this process, each joint is tracked through its full range of motion and results in an array of points within the workspace of the given mechanism. Fig. 5 and 6 show the individual workspaces of the user interface and spatial force feedback mechanism with respect to the global coordinate frame of the haptic device.

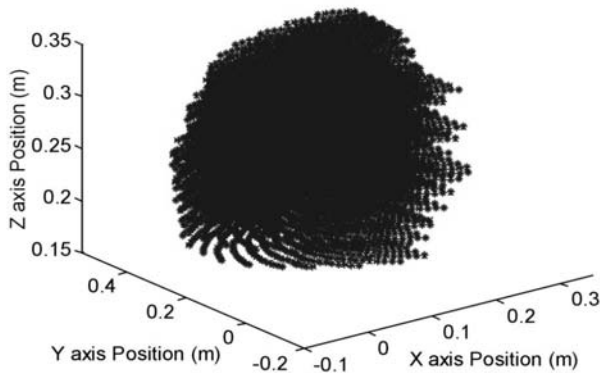


Figure 5: Workspace of the user interface in the global coordinate frame.

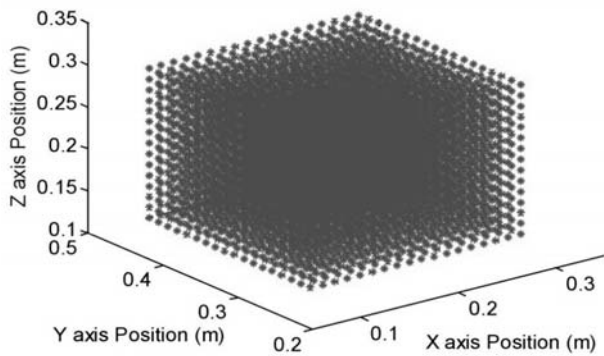


Figure 6: Workspace of the spatial mechanism in the global coordinate frame.

Next, we take the intersection of the workspaces of both halves to obtain the reachable workspace of the haptic device. This is achieved by taking the boundary of the spatial mechanism's workspace and finding all the points from the user interface's workspace that are within this boundary. Fig. 7 shows the reachable workspace of the device. This reachable workspace represents an estimated volume of 0.0041 cubic meters with dimensions of approximately 0.1905m wide by 0.1905m deep by

0.1143m high. An algorithm was developed for volume estimation that discretizes the achievable workspace and determines which 3D elements are located in the workspace.

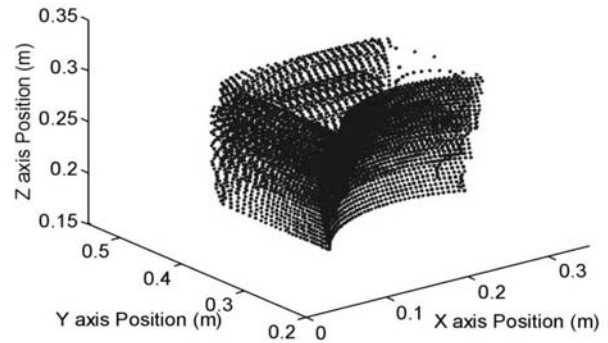


Figure 7: Reachable workspace of the haptic device.

3 FRICTION ESTIMATION

To increase transparency of the haptic device, it is necessary to estimate the friction in the various actuated joints. Therefore, estimation of accurate friction in a haptic device is necessary for improving the overall performance of the device. While using precision machined parts, bearings, cable transmissions, and other lower friction options for the actuators and joints can help reduce friction, it is impossible to eliminate it altogether. However, by using a feed forward controller that can power the actuators to overcome the friction in the mechanism, an essentially "frictionless" device can be achieved.

To develop a highly transparent haptic device, we measured the required voltage to the motor to produce a very low velocity movement of the joint. Therefore, we commanded each motor on the spatial mechanism (X, Y, and Z axes) through its full range of motion with a voltage where the motion of the axis was with a very low velocity (approximately 0.0025m/sec). This voltage value for each position along the axis was then taken to be the friction voltage required for our feedforward model. This friction calculation was performed on the three axes for both the forward and reverse direction. The voltage was sampled at 1000Hz and then fed-forward in the controller through the use of a look-up table. Through appropriate calibration, this friction voltage was converted to the friction torque necessary to overcome the friction along each axis of motion. Each motor uses an amplifier to convert an input voltage to a proportional current to power the motor. Therefore, the friction voltage, which is the voltage sent to the amplifier from the computer, can be converted to the proportional friction torque through the torque constant and applied current by the amplifier to the motor. Fig. 8 shows the friction torque measured over the full range of each axis for both the forward and reverse motion. As shown in the figure, the friction torque varies over the range of motion with the maximum friction torque of 32 mNm, which is approximately 17.6% of the maximum motor torque (181mNm).

In addition to the spatial mechanism, we measured the friction in the grasping mechanism (θ) using the same method as in the spatial mechanism. The results are shown in fig. 9. The maximum friction measured for the grasping mechanism was 24

mNm, which is approximately 27% of the maximum motor torque (88.8mNm).

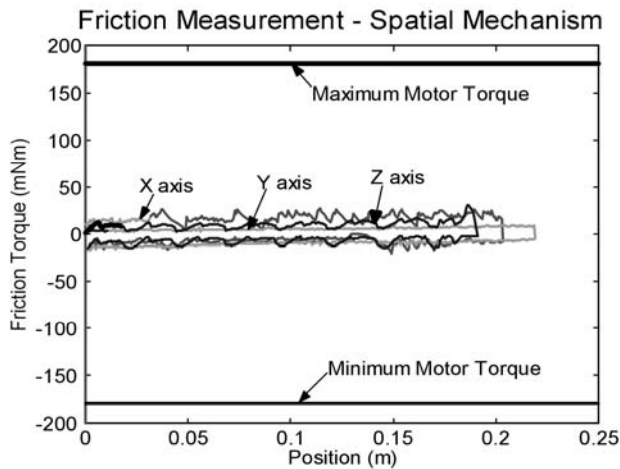


Figure 8: Friction measured along the axes of the spatial force feedback mechanism.

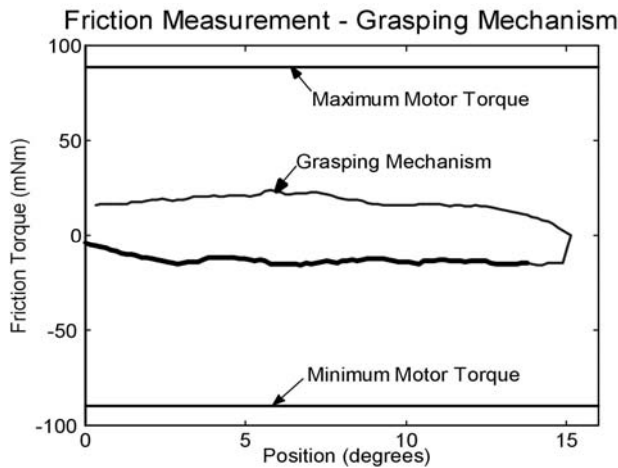


Figure 9: Friction measured along the angular position of the grasping mechanism.

4 DISCUSSION

We have presented our 7 DOF haptic device that consists of a closed kinematic chain with a user interface and a spatial force feedback mechanism. This device was designed with applications in robot-assisted MIS and other areas, such as the automotive industry, gaming industry, rehabilitation aid for people with finger, hand, and/or forearm injuries, etc. We have also presented the kinematic analysis of the mechanism in calculation of the reachable workspace. Furthermore, a friction estimation of the actuated joints has also been presented.

Future work includes the implementation of the friction estimation measurements in a feed-forward controller as a friction compensator. Additional future work includes using the haptic device to control the position and orientation of the end point laparoscopic tool attached to the end-effector of a slave robot arm for soft-tissue telemanipulation experiments.

ACKNOWLEDGMENT

We would like to acknowledge the support of National Science Foundation grants: EIA-0312709 and CAREER Award IIS-0133471 for this work.

REFERENCES

- [1] K. Vlachos, E. Papadopoulos, and D. N. Mitropoulos, "Design and Implementation of a Haptic Device for Training in Urological Operations," *IEEE Transactions on Robotics and Automation*, vol. 19, pp. 801-809, 2003.
- [2] R. Baumann, W. Maeder, D. Glauser, and R. Clavel, "The Pantoscope: A Spherical Remote-Center-of-Motion Parallel Manipulator for Force Reflection," presented at IEEE International Conference on Robotics and Automation, Albuquerque, New Mexico, 1997.
- [3] S. Payandeh and T. Li, "Towards new designs of haptic devices for minimally invasive surgery," *International Congress Series*, pp. 775-781, 2003.
- [4] V. Hayward, P. Gregorio, O. Astley, S. Greenish, and M. Doyon, "Freedom-7: A High Fidelity Seven Axis Haptic Device With Application to Surgical Training," *Experimental Robotics VI*, pp. 445-456, 1998.
- [5] E. Papadopoulos, K. Vlachos, and D. Mitropoulos, "Design of a 5-dof Haptic Simulator for Urological Operations," presented at IEEE International Conference on Robotics and Automation, Washington, DC, 2002.
- [6] A. Bicchi, G. Canepa, D. DeRossi, P. Iacconi, and E. Scilingo, "A sensor-based minimally invasive surgery tool for detecting tissue elastic properties," presented at IEEE International Conference on Robotics and Automation, 1996.
- [7] J. Dargahi, M. Parameswaran, and S. Payandeh, "A Micromachined Piezoelectric Tactile Sensor for an Endoscopic Grasper - Theory, Fabrication and Experiments," *Journal of Microelectromechanical Systems*, vol. 9, pp. 329-335, 2000.
- [8] V. V. H. t. Dingshoft, M. Lazeroms, A. v. d. Ham, W. Jongkind, and G. Hondred, "Force reflection for a laparoscopic forceps," presented at 18th Annual International Conference of the IEEE Engineering in Medicine and Biology Society, 1996.
- [9] T. Hu, A. E. Castellanos, G. Tholey, and J. P. Desai, "Real-Time Haptic feedback in Laparoscopic tool for use in Gastro-intestinal Surgery," presented at Fifth International Conference on Medical Image Computing and Computer Assisted Intervention (MICCAI), 2002.
- [10] A. J. Madhani, G. Niemeyer, and J. K. Salisbury, "The Black Falcon: A Teleoperated Surgical Instrument for Minimally Invasive Surgery," *IEEE/RSJ International Conference on Intelligent Robotic Systems*, vol. 2, pp. 936-944, 1998.
- [11] V. F. Munoz, C. Vara-Thorbeck, et al., "A medical robotic assistant for minimally invasive surgery," presented at IEEE International Conference on Robotics and Automation, 2000.
- [12] D. T. V. Pawluk, J. S. Son, P. S. Wellman, W. J. Peine, and R. D. Howe, "A Distributed Pressure Sensor for Biomechanical Measurements," *ASME Journal of Biomechanical Engineering*, vol. 102, pp. 302-305, 1998.
- [13] J. Rosen, B. Hannaford, M. MacFarlane, and M. Sinanan, "Force Controlled and Teleoperated Endoscopic Grasper for Minimally Invasive Surgery - Experimental Performance Evaluation," *IEEE Transactions on Biomedical Engineering*, vol. 46, pp. 1212-1221, 1999.
- [14] D. Salle, F. Gosselin, P. Bidaud, and P. Gravez, "Analysis of haptic feedback performances in telesurgery robotic systems," presented at IEEE International workshop on Robot and Human Interactive Communication, 2001.
- [15] E. Scilingo, D. DeRossi, A. Bicchi, and P. Iacconi, "Sensor and devices to enhance the performance of a minimally invasive

- surgery tool for replicating surgeon's haptic perception of the manipulated tissues," presented at IEEE International Conference on Engineering in Medicine and Biology, 1997.
- [16] G. Tholey, A. Pillarisetti, and J. P. Desai, "On-Site Three Dimensional Force Sensing Capability in a Laparoscopic Grasper," *Industrial Robot*, vol. 31, pp. 509-518, 2004.
- [17] M. Tavakoli, R. V. Patel, and M. Moallem, "A Forcec Reflective Master-Slave System for Minimally Invasive Surgery," presented at IEEE International Conference on Intelligent Robots and Systems, Las Vegas, Nevada, 2003.
- [18] R. H. Taylor, J. Funda, et al., "A telerobotic assistant for laparoscopic surgery," *IEEE Engineering in Medicine and Biology*, vol. 14, pp. 279-286, 1995.
- [19] G. Tholey and J. P. Desai, "A General Purpose 7 DOF Haptic Interface," presented at First Joint Eurohaptics Conference and Symposium on Haptic Interfaces for Virtual Environment and Teleoperator Systems, Pisa, Italy, 2005.
- [20] G. Tholey, A. Pillarisetti, W. Green, and J. P. Desai, "Design, Development, and Testing of an Automated Laparoscopic Grasper with 3-D Force Measurement Capability," presented at Second International Symposium on Medical Simulation Emerging Science|Enabling Technologies, Boston, MA, 2004.
- [21] J. Rosen, M. MacFarlane, C. Richard, B. Hannaford, and M. Sinanan, "Surgeon-Tool Force/Torque Signatures - Evaluation of Surgical Skills in Minimally Invasive Surgery," presented at Medicine Meets Virtual Reality, San Francisco, CA, 1999.
- [22] V. Gupta, N. P. Reddy, and P. Batur, "Forces in Surgical Tools: Comparison between Laparoscopic and Surgical Forceps," presented at International Conference of the IEEE Engineering in Medicine and Biology Society, Amsterdam, 1996.